Research Article Vol. 29, No. 2 / 18 January 2021 / Optics Express 1289
Optics EXPRESS

Two-dimensional grating coupler on an X-cut lithium niobate thin-film

BIN CHEN,[1] ZILIANG RUAN,[1] JINYAO HU,[2] JINGYI WANG,[2] CHAO LU,[3] ALAN PAK TAO LAU,[4] CHANGJIAN GUO,[2] KAIXUAN CHEN,[2,5] PENGXIN CHEN,[2] AND LIU LIU[1,6]

[1]*State Key Laboratory for Modern Optical Instrumentation, Centre for Optical & Electromagnetic Research, College of Optical Science and Engineering, International Research Center for Advanced Photonics, East Building No. 5, Zijingang Campus, Zhejiang University, Hangzhou 310058, China*
[2]*Centre for Optical and Electromagnetic Research, Guangdong Provincial Key Laboratory of Optical Information Materials and Technology, South China Academy of Advanced Optoelectronics, Sci. Bldg. No. 5, South China Normal University, Higher-Education Mega-Center, Guangzhou 510006, China*
[3]*Photonics Research Center, Department of Electronic and Information Engineering, The Hong Kong Polytechnic University, Hong Kong SAR, China*
[4]*Photonics Research Center, Department of Electrical Engineering, The Hong Kong Polytechnic University, Hong Kong SAR, China*
[5]*chenkaixuan@m.scnu.edu.cn*
[6]*liuliuopt@zju.edu.cn*

Abstract: A two-dimensional grating coupler for coupling light between a standard single-mode fiber and ridge waveguides on an X-cut lithium niobate thin-film is designed and demonstrated. Using circular holes for grating cells, simulated coupling losses reach −3.88 dB at 1550 nm and −5.78 dB at 1563 nm with 1-dB bandwidths of 49 nm and 45 nm for P-polarized and S-polarized light inputs, respectively. Experimentally, peak coupling losses of −5.13 dB at 1561 nm and −7.6 dB at 1568 nm are obtained for P-polarized and S-polarized light inputs, respectively, and corresponding 1 dB bandwidths are about 30 nm. An approach to improve the coupling performance of the grating coupler is also proposed using two crossing ellipses as grating cells as well as a bottom metal reflector. The coupling loss and the polarization dependent loss are decreased to around −3.4 dB and 0.44 dB, respectively.

1. Introduction

Lithium niobate (LN) is a versatile material for optical integration due to its outstanding properties including wide transparency window, large refractive index, and excellent electro-optic, acousto-optic, nonlinear coefficients [1]. Conventionally, an LN waveguide is fabricated using titanium diffusion or proton exchange. These types of waveguides have weak optical confinement and thus are unsuitable for densely integrated circuits. Recently, a new type of wafer structure, i.e., LN on insulator (LNOI), emerges and draws great interests. By bonding an LN thin-film of a sub-micron thickness on a silica buffer layer, the LNOI structure exhibits a high refractive index contrast and thus can accommodate waveguides with strong optical confinement, as well as a low loss [2]. So far, many photonic devices with excellent performances have been realized, including microring/microdisk resonators [3,4], photonic crystal cavities [5], electro-optic modulators [6,7], frequency comb devices [8], etc.

Although the on-chip functionalities based on LNOI are developing, a low loss optical interface from a fiber to an LNOI waveguide is still challenging. The size of a typical ridge waveguide on LNOI is below one micron, which is much less than the mode field size of a standard single-mode fiber (SMF). Therefore, a high coupling loss may occur due to the large mode mismatch [1,2]. Inverse taper based edge couplers or grating couplers can be employed to solve this problem.

#413820 https://doi.org/10.1364/OE.413820
Journal © 2021 Received 2 Nov 2020; revised 20 Dec 2020; accepted 21 Dec 2020; published 7 Jan 2021

Optics EXPRESS

Inverse taper couplers facilitate a high coupling efficiency and a wide working wavelength range [9–11]. The best reported coupling loss of such couplers so far reached −1.32 dB [11]. However, the tiny tip end needed in this type of coupler is still challenging to fabricate on LNOI due to non-vertical side-walls resulted from the LN etching [9]. Additionally, inverse taper couplers can be only used at chip edges. Grating couplers, on the other hand, are more versatile considering their advantages of flexible layout, wafer scale testing, and large alignment tolerance. On the LNOI platform discussed here, one dimensional grating couplers (1D GCs) have been extensively studied [12–20], among which the coupling loss of −3.06 dB with a 1-dB bandwidth of 55 nm has been demonstrated so far [15]. It is worth noting that 1D GCs normally work for only one polarization. Yet, two-dimensional grating couplers (2D GCs), considered as two 1D GCs orthogonally positioned, can couple the input light of an arbitrary polarization to its two arms with the same polarization. It is also one key element for building polarization diversity circuits [21]. During recent years, high performance 2D GCs have been developed on the Silicon-on-Insulator (SOI) platform with high coupling efficiencies and low polarization dependent losses (PDLs) [22–27]. Despite its success on SOI, a 2D GC on LNOI is still missing so far.

In this paper, we demonstrate a 2D GC with circular grating patterns on LNOI. Theoretically, optimized peak coupling losses are −3.88 dB at 1550 nm for the P-polarized light input and −5.78 dB at 1563 nm for the S-polarized light input. Their 1-dB coupling bandwidths are 49 nm and 45 nm, respectively. Experimentally, −5.13 dB and −7.6 dB peak coupling losses are demonstrated for the two polarizations, respectively. Measured 1-dB coupling bandwidths are ~30 nm. Also, we propose an approach to improve the coupling efficiency and PDL performance by using two crossing ellipses as grating cells and a bottom metal reflector on the LNOI wafer.

2. Design

The schematic structure of the proposed 2D GC and its cross-sectional view are presented in Fig. 1. The LNOI wafer structure consists of an LN slab, a buried oxide (BOX) layer, and a silicon substrate. Waveguides and patterns of grating scatters, which are arranged in square, are etched in the LN slab. Two linear tapers are used to connect the respective ports of the 2D GC to a single mode LN ridge waveguide. The symmetric plane of the present structure is also indicated in Fig. 1(a). A fiber is placed on top of the GC within the symmetry plane. It is tilted for −10 degrees with respect to the normal direction of the chip surface. Two polarization states of the input light, i.e., P-polarization (electric field parallel to the symmetry plane) and S-polarization (electric field perpendicular to the symmetry plane), are used to evaluate the coupling efficiency and the PDL of the GC. Here, the PDL is defined as the absolute value of the difference between the coupling spectra of P-polarized and S-polarized light inputs. As shown in Fig. 1(b), the LNOI wafer that we adopted here has a $t = 400$ nm thick LN layer on top of a $b = 3$ μm thick BOX layer. Circular grating scatters have a period of p and a diameter of d, measured at the central depth of the hole. Their etching depth e are the same as that of the LN ridge waveguides. The side wall angle (SWA) of all etched LN patterns are assumed 60°, which is a typical value from the current fabrication technology.

A three-dimensional finite-difference time-domain algorithm is employed to optimize the proposed 2D GC. In order to simulate the SMF, a Gaussian beam with a waist diameter of 10.4 μm is input from top of the grating with an incident angle of −10 degrees as discussed above. The coupling efficiency is calculated as the total transmission to the fundamental transverse electrical (TE) mode in the two LN ridge waveguides. The etching depth e is 200 nm, which is one half of the total LN layer thickness. Then, the period p and the diameter d of the grating scatters are the remaining parameters needed to optimize. For convenience, we use duty cycle dc, instead of d, for optimization. Here, dc is defined as the area percentage of the etched hole within one grating period, i.e., $dc = \pi(d/2)^2/p^2$. We sweep p and dc while monitoring the coupling efficiency with a P-polarized light input. The results are presented in Fig. 2(a). The optimal

Optics EXPRESS

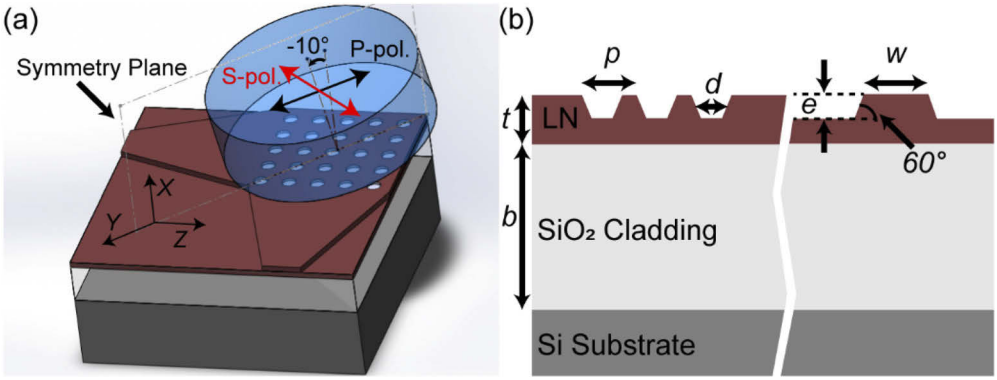

Fig. 1. (a) Schematic structure of the proposed 2D GC. (b) Cross-sectional view of the grating and the waveguide on the LNOI structure.

position, i.e., $p = 849$ nm and $dc = 0.5$ ($d = 338$ nm), where the transmission reaches the peak, is marked with an asterisk. Figure 2(b) shows the coupling spectra of the optimal structure. Here, the best coupling loss reaches −3.88 dB at 1550 nm for the P-polarized light input and −5.78 dB at 1563 nm for the S-polarized light input. The 1-dB coupling bandwidths are 49 nm and 45 nm, respectively. The PDL is relatively large, i.e., 2.17dB at 1550nm.

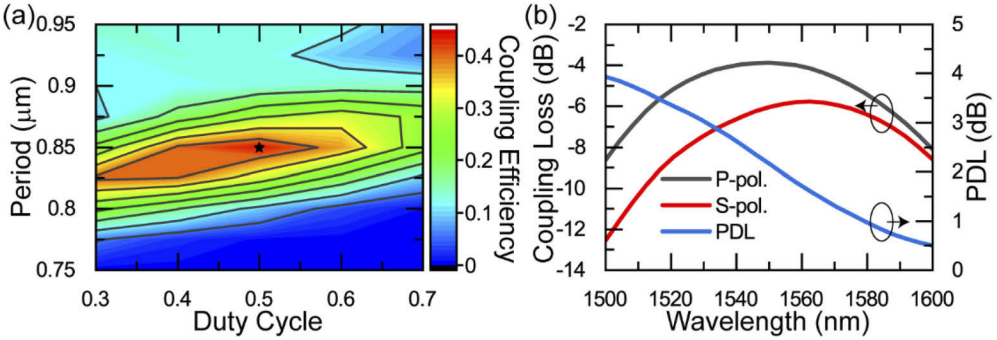

Fig. 2. (a) Contour plot of the coupling efficiency at 1550 nm wavelength for the P-polarized light input for various structural parameters. (b) Simulated coupling spectra, as well as PDLs, of the optimized 2D GC for P-polarized and S-polarized light inputs. The values of period p and duty cycle dc are taken from the asterisk position in (a).

The fabrication tolerance of the 2D GC was further investigated. Since the period p of the grating can be defined rather accurately using modern fabrication technologies, we have then varied the hole diameter d, the etching depth e, and the SWA separately on the optimized structure. Simulated coupling spectra are shown in Fig. 3. For sweeping SWA, the volume of each etched grating hole is kept constant. One can find that the peak coupling wavelength are relatively insensitive to the SWA for both polarizations. For the hole diameter, ±60 nm variations in d would result in ∓13 nm shifts of the peak coupling wavelength. The peak coupling efficiency is however insensitive to Δd. The etching depth, on the other hand, poses a greater impact on both coupling efficiency and wavelength. The peak coupling loss varies for 0.62 dB for the P-polarized input and 0.7 dB for the S-polarized input, when e changes for 60 nm. The peak coupling efficiency tends to increase when the grating holes are etched more deeply. This implies that 200 nm is not the optimal etching depth for the present grating coupler. Yet, in order to be

Optics EXPRESS

compatible to other devices on LNOI, such as modulators which are normally etched by one half of the total LN thickness [7], $e = t/2 = 200$ nm is still adopted throughout the paper.

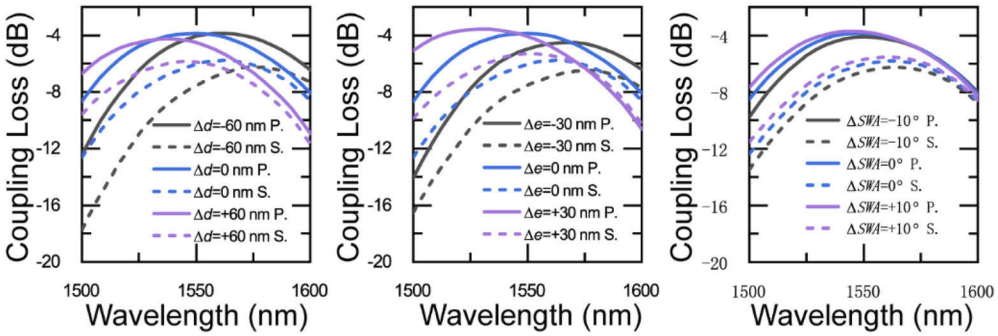

Fig. 3. Impacts of the variations in (a) hole diameter d, (b) etching depth e, and (c) SWA on the coupling loss.

In the previous design, the coupling spectra of the two polarizations are different in both peak coupling losses and wavelengths, which leads to large PDLs. In our earlier work for a 2D GC on SOI [27], we have proven that central wavelengths of the two coupling spectra can be made coincide by using two crossing ellipses as grating cells. This approach is also applied in the present structure as shown in Fig. 4(a). Through a series of simulations, optimized parameters in this type of structure are found to be $r_L = 972$ nm, $r_S = 476$ nm, and $p = 845$ nm. Here, we further use a gold mirror just above the silicon substrate to improve the coupling efficiency. The BOX layer thickness b was thereby swept, and the resulting coupling efficiencies for the two polarizations at 1550 nm wavelength are plotted in Fig. 4(b). As expected, periodic oscillations due to interference are presented. However, the maximal values and the corresponding BOX layer thicknesses are different for P-polarized and S-polarized light inputs. Nevertheless, we can choose a suitable b for a better PDL without largely compromising the coupling efficiency. Here, $b = 2.58$ μm is adopted, and the full coupling spectra, as well as PDLs, in this case is shown in Fig. 4(c). As compared to the structure in Fig. 1, the PDLs in the present structure are greatly improved to < 0.44 dB within the entire simulated wavelength band. At the same time, peak

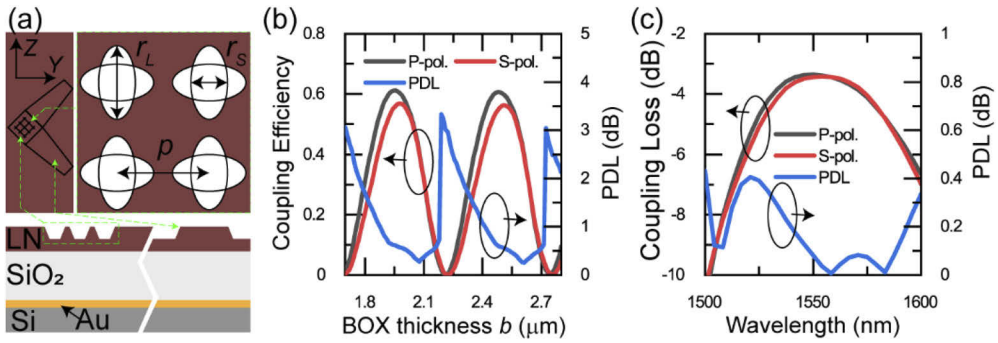

Fig. 4. (a) Schematic structure of the 2D GC with two crossing ellipses as grating cells. (b) Simulated coupling efficiencies of P-polarized and S-polarized light inputs as a function of the BOX layer thickness b at 1550 nm wavelength, and maximal PDLs within the 1-dB coupling bandwidth. (c) Coupling losses of the two polarizations and the corresponding PDLs at $b = 2.58$ μm.

Optics EXPRESS

coupling losses are also improved to −3.36 dB and −3.42 dB for P-polarized and S-polarized light inputs, respectively.

3. Fabrication and measurement

Due to the wafer available at hand, the first 2D GC with circular grating patterns without the gold reflection mirror was fabricated. the LNOI wafer with $t = 400$ nm and $b = 3$ μm was purchased from Jinan Jingzheng Electronics Co., Ltd. The grating patterns, as well as the ridge waveguides, were defined in an ma-N 2403 resist layer on top of the LNOI chip using electron beam lithography. Inductively-coupled-plasma reactive-ion etching (RIE) process was used to transfer the resist pattern to the LN layer. Here, the grating and waveguide structures were fabricated using one etching step. Optical and scan-electron microscope pictures of one finished sample are displayed in Fig. 5. Two linear tapers of 250 μm long are attached to the 2D GC for adiabatic coupling to two single-mode LN ridge waveguides of 1.5 μm width. At the other ends, two 1D GCs for TE mode were prepared for light out-coupling.

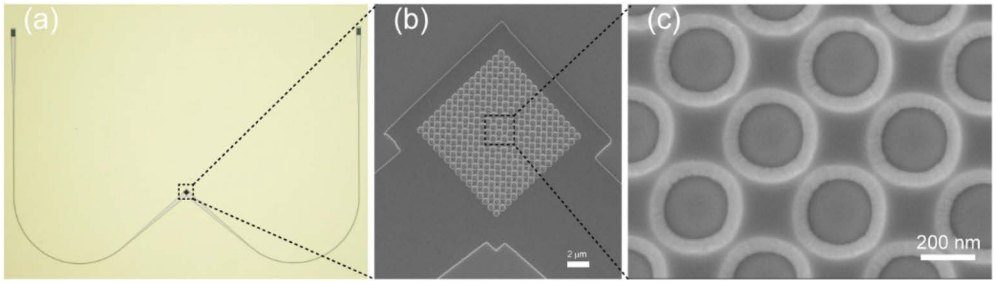

Fig. 5. (a) Optical microscope picture of the fabricated structure. Scan-electron microscope pictures of (b) 2D GC and (c) zoom-in view of grating scatters.

A broad-band super luminescent diode and an optical spectrum analyzer were used to test the spectral responses of fabricated devices. The response of the out-coupling 1D GC was first measured using a structure with two such 1D GCs connected back to back. For measuring the 2D GC, the polarization state of the input light was adjusted to either P or S polarization. In order to count the final coupling efficiency of a 2D GC, the light powers measured from the two out-coupling 1D GCs were summed after normalizing out the coupling loss of the 1D GC. The

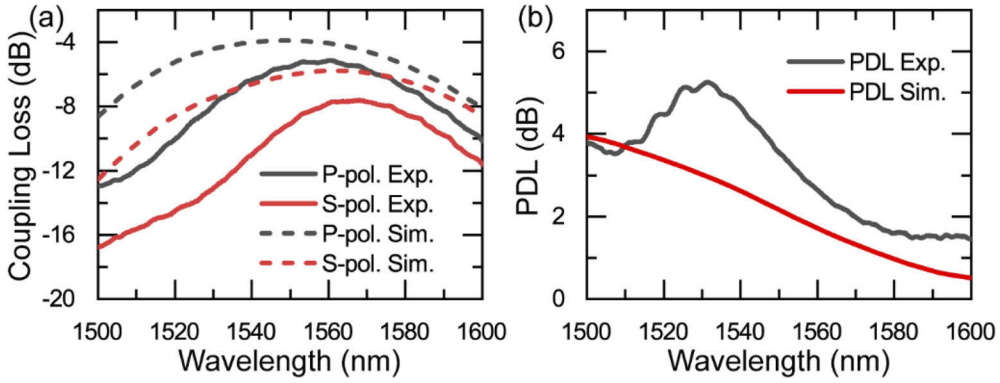

Fig. 6. (a) Measured and simulated coupling spectra of the 2D GC for P-polarized and S-polarized light inputs and (b) corresponding PDLs.

Optics EXPRESS

LN ridge waveguides connecting the grating couplers were considered lossless as the measured propagation losses are small, i.e., ~1 dB/cm [6]. Figure 6 shows measured coupling spectra of a fabricated 2D GC. The best coupling loss of −5.13 dB is obtained for the P-polarized light input at 1561 nm wavelength, and −7.6 dB for the S-polarized light input at 1568 nm. Their 1-dB bandwidths are 32 nm and 29 nm, respectively. Compared to simulation results shown in the same figure, the peak coupling wavelengths of the measured spectra exhibit red shifts. The peak coupling losses are also higher than the simulated ones by 1.25 dB and 1.82 dB for P-polarized and S-polarized light inputs, respectively. According to Fig. 3(b), these deviations probably resulted from the inadequate etching depth of the grating holes as compared to that of the waveguides due to, e.g., the RIE lag effect.

4. Conclusion

We have designed and demonstrated a 2D GC on the LNOI platform by directly etching the LN layer to form the grating and the waveguides. Peak coupling losses of −3.88 dB at 1550 nm wavelength for the P-polarized light input and −5.78 dB at 1563 nm for the S-polarized light input are obtained theoretically for an optimized structure using circular grating scatters. Corresponding 1-dB bandwidths are 49 nm and 45 nm, respectively. Experimentally, the fabricated sample exhibits peak coupling losses of −5.13 dB and −7.6 dB for the two polarization, respectively, with slightly red-shifted peak coupling wavelengths. The measured 1-dB bandwidths are ~30 nm. We have also proposed an approach to improve the coupling efficiency as well as PDLs by using two crossing ellipses as grating cells and a bottom metal reflector on an LNOI structure with an optimized BOX layer thickness. This kind of LNOI wafer is also commercially available. With this approach, the coupling loss and the PDL have been decreased to around −3.4 dB and 0.44 dB, respectively.

Funding. National Major Research and Development Program (2019YFB1803902); National Natural Science Foundation of China (61675069); Science and Technology Planning Project of Guangdong Province (2019A050510039).

Disclosures. The authors declare no conflicts of interest.

References

1. Y. Qi and Y. Li, "Integrated lithium niobate photonics," Nanophotonics **9**(6), 1287–1320 (2020).
2. A. Boes, B. Corcoran, L. Chang, J. Bowers, and A. Mitchell, "Status and Potential of Lithium Niobate on Insulator (LNOI) for Photonic Integrated Circuits," Laser Photonics Rev. **12**(4), 1700256 (2018).
3. A. Guarino, G. Poberaj, D. Rezzonico, R. Degl'Innocenti, and P. Gunter, "Electro-optically tunable microring resonators in lithium niobate," Nat. Photonics **1**(7), 407–410 (2007).
4. C. Wang, M. J. Burek, Z. Lin, H. A. Atikian, V. Venkataraman, I. C. Huang, P. Stark, and M. Loncar, "Integrated high quality factor lithium niobate microdisk resonators," Opt. Express **22**(25), 30924–30933 (2014).
5. H. Liang, R. Luo, Y. He, H. W. Jiang, and Q. Lin, "High-quality lithium niobate photonic crystal nanocavities," Optica **4**(10), 1251–1258 (2017).
6. M. He, M. Xu, Y. Ren, J. Jian, Z. Ruan, Y. Xu, S. Gao, S. Sun, X. Wen, L. Zhou, L. Liu, C. Guo, H. Chen, S. Yu, L. Liu, and X. Cai, "High-performance hybrid silicon and lithium niobate Mach-Zehnder modulators for 100 Gbit s(-1) and beyond," Nat. Photonics **13**(5), 359–364 (2019).
7. C. Wang, M. Zhang, X. Chen, M. Bertrand, A. Shams-Ansari, S. Chandrasekhar, P. Winzer, and M. Loncar, "Integrated lithium niobate electro-optic modulators operating at CMOS-compatible voltages," Nature **562**(7725), 101–104 (2018).
8. M. Zhang, B. Buscaino, C. Wang, A. Shams-Ansari, C. Reimer, R. Zhu, J. M. Kahn, and M. Loncar, "Broadband electro-optic frequency comb generation in a lithium niobate microring resonator," Nature **568**(7752), 373–377 (2019).
9. I. Krasnokutska, J. L. J. Tambasco, and A. Peruzzo, "Nanostructuring of LNOI for efficient edge coupling," Opt. Express **27**(12), 16578–16585 (2019).
10. L. He, M. Zhang, A. Shams-Ansari, R. Zhu, C. Wang, and L. Marko, "Low-loss fiber-to-chip interface for lithium niobate photonic integrated circuits," Opt. Lett. **44**(9), 2314–2317 (2019).
11. N. Yao, J. Zhou, R. Gao, J. Lin, M. Wang, Y. Cheng, W. Fang, and L. Tong, "Efficient light coupling between an ultra-low loss lithium niobate waveguide and an adiabatically tapered single mode optical fiber," Opt. Express **28**(8), 12416–12423 (2020).
12. Z. Chen, R. Peng, Y. Wang, H. Zhu, and H. Hu, "Grating coupler on lithium niobate thin film waveguide with a metal bottom reflector," Opt. Mater. Express **7**(11), 4010–4017 (2017).

Optics EXPRESS

13. M. S. Nisar, X. Zhao, A. Pan, S. Yuan, and J. Xia, "Grating Coupler for an On-Chip Lithium Niobate Ridge Waveguide," IEEE Photonics J. **9**(1), 1–8 (2017).
14. Z. Chen, Y. Wang, H. Zhang, and H. Hu, "Silicon grating coupler on a lithium niobate thin film waveguide," Opt. Mater. Express **8**(5), 1253–1258 (2018).
15. J. Jian, P. Xu, H. Chen, M. He, Z. Wu, L. Zhou, L. Liu, C. Yang, and S. Yu, "High-efficiency hybrid amorphous silicon grating couplers for sub-micron-sized lithium niobate waveguides," Opt. Express **26**(23), 29651–29658 (2018).
16. A. Kar, M. Bahadori, S. Gong, and L. L. Goddard, "Realization of alignment-tolerant grating couplers for z-cut thin-film lithium niobate," Opt. Express **27**(11), 15856–15867 (2019).
17. I. Krasnokutska, R. J. Chapman, J. L. J. Tambasco, and A. Peruzzo, "High coupling efficiency grating couplers on lithium niobate on insulator," Opt. Express **27**(13), 17681–17685 (2019).
18. Z. Chen, Y. Ning, and Y. Xun, "Chirped and apodized grating couplers on lithium niobate thin film," Opt. Mater. Express **10**(10), 2513–2521 (2020).
19. C. C. Kores, M. Fokine, and F. Laurell, "UV-written grating couplers on thin-film lithium niobate ridge waveguides," Opt. Express **28**(19), 27839–27849 (2020).
20. X. Ma, C. Zhuang, R. Zeng, J. J. Coleman, and W. Zhao, "Polarization-independent one-dimensional grating coupler design on hybrid silicon/LNOI platform," Opt. Express **28**(11), 17113–17121 (2020).
21. D. Taillaert, H. Chong, P. I. Borel, L. H. Frandsen, R. M. De La Rue, and R. Baets, "A compact two-dimensional grating coupler used as a polarization splitter," IEEE Photonics Technol. Lett. **15**(9), 1249–1251 (2003).
22. L. Carroll, D. Gerace, I. Cristiani, and L. C. Andreani, "Optimizing polarization-diversity couplers for Si-photonics: reaching the -1 dB coupling efficiency threshold," Opt. Express **22**(12), 14769–14781 (2014).
23. J. Zou, Y. Yu, and X. Zhang, "Single step etched two dimensional grating coupler based on the SOI platform," Opt. Express **23**(25), 32490–32495 (2015).
24. J. Zou, Y. Yu, and X. Zhang, "Two-dimensional grating coupler with a low polarization dependent loss of 0.25 dB covering the C-band," Opt. Lett. **41**(18), 4206–4209 (2016).
25. T. Watanabe, Y. Fedoryshyn, and J. Leuthold, "2-D Grating Couplers for Vertical Fiber Coupling in Two Polarizations," IEEE Photonics J. **11**(4), 1–9 (2019).
26. Y. Xue, H. Chen, Y. Bao, J. Dong, and X. Zhang, "Two-dimensional silicon photonic grating coupler with low polarization-dependent loss and high tolerance," Opt. Express **27**(16), 22268–22274 (2019).
27. B. Chen, X. Zhang, J. Hu, Y. Zhu, X. Cai, P. Chen, and L. Liu, "Two-dimensional grating coupler on silicon with a high coupling efficiency and a low polarization-dependent loss," Opt. Express **28**(3), 4001–4009 (2020).